INSIGHTS INTO THE BREAKAGE BEHAVIOUR AND BREAKAGE MECHANISM OF GIBBSITE DURING CALCINATION

J. Zhang,[1] Z. Chen,[2] L. Ge,[1] E. Boom,[3] Z. Zhu[1*]

[1]*School of Chemical Engineering, The University of Queensland, Brisbane 4072 Australia*

[2]*School of Mechanical and Mining Engineering, The University of Queensland*

[3]*Technology and Improvement, South32, Collie, WA 6225*

**Corresponding author: z.zhu@uq.edu.au*

ABSTRACT

Breakdown of gibbsite particles during calcination is one of the main contributor to superfines in smelter grade alumina. Understanding the breakage behaviour and mechanism can guide the controlling of superfine generation. Extensive work has been carried out to characterise SGA's breakage, yet key challenge remains in understanding the breakage behaviour and mechanism.

In this study, internal morphology change of calcined gibbsite was studied by focus iron beam (FIB) – scanning electron microscope (SEM) and 3D tomographic images by phase segmentation. The formation of internal cracks at the bulk phase were found on particles without surface cracks. These results indicate that cracks are initiated in the bulk of crystallite, and grow towards the surface.

1. INTRODUCTION

In the aluminium production process, a series of problems can be caused by the existence of ultra-fine particles existing in its raw material, smelter grade alumina (SGA). The ultra-fine particles' generation attribute to the breakage of gibbsite during calcination happens in preparing SGA, therefore understanding the breakage behaviour and mechanism of gibbsite breakage is of potential help to limit the breakage of gibbsite in calcination.

A series of research have been done on the breakage of gibbsite in calcination. The breakage of the gibbsite crystallite during calcination is usually reckoned to be motivated by c-axis shrinkage of crystallites during calcination[1]. Factors including the calcination methods, the morphology of SGA as well as the transition and storage condition are considered to have influence on the SGA breakage condition [2-7]. The breakage happens to gibbsite are previously observed and researched in many works[2, 5-6, 8-10], yet the mechanism of gibbsite crystallites requires further research.

In this paper, in order to find out the linkage between the phase conversion and breakage on gibbsite crystallite surface, we compared the crystal phase content analysed by X-ray diffraction (XRD) and the crack width measured and counted in SEM images in gibbsite calcined at different temperature. In order to understand the mechanism of gibbsite breakage, we observed the internal morphology of calcined gibbsite crystallite by focus iron beam (FIB) based SEM and compared it with the surface. The gibbsite crystallite breakage was found to initiate from pores generated inside the internal part of the crystallite then grow to form strip-like cracks. Some of these cracks grow through the surface and form open cracks observed on the crystallite surface.

2. EXPERIMENTAL

Commercial gibbsite provided by South 32 Worsley Alumina Pty Ltd. was calcined with a ramping rate of 10ºC • min^{-1} at 260ºC, 450ºC and 470ºC respectively. The samples were maintained at the targeted temperature for 5 hours in static air then naturally cooled down to room temperature.

The samples were analysed by a Rigaku smartlab thin-film and micro-diffraction XRD. The surface of these samples was observed by an SEM (JEOL 7001) and the cracks' width in each sample was counted by Image J.

In order to propose the mechanism of gibbsite breakage during calcination, we applied an FEI SCIOS FIB/SEM duel beam focus iron beam (FIB) system to observe the internal morphology change of

the crystallites. We also built a 3D model of the distribution of cracks in the crystallite by FIB 3D tomography.

3. RESULTS AND DISCUSSION

The XRD patterns of gibbsite before calcination and calcined at different temperature are shown in Figure 1. It is found that the major component of sample converted from gibbsite to boehmite at 260ºC. The boehmite phase maintained till 470ºC, when it changed to amorphous alumina.

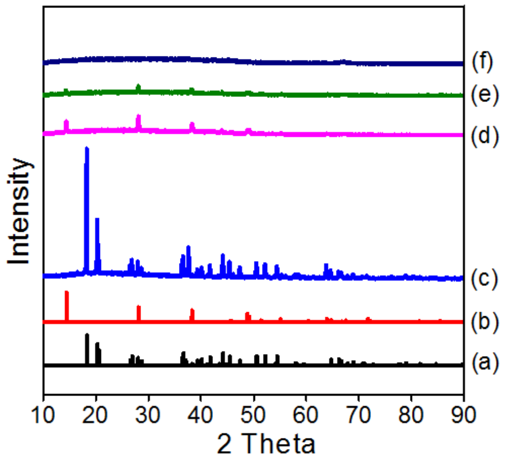

Figure 1. Standard pattern of (a) gibbsite (b) boehmite and XRD patterns of sample (c) before calcination (d) calcined at 260ºC (e) calcined at 450ºC (f) calcined at 470ºC

To find out the linkage between phase conversion and breakage of gibbsite surface, we measured and collected the width of cracks in SEM images and made comparison with the phase conversion process found in XRD patterns. The SEM image of gibbsite surface and the crack width distribution of different samples are given in Figure 2 and Figure 3 respectively.

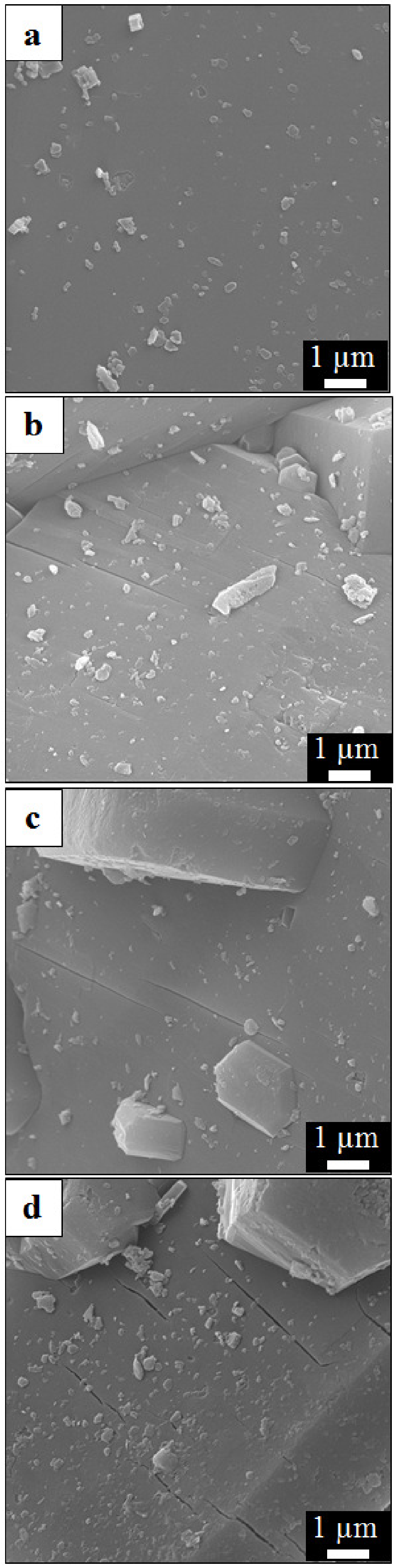

Figure 2. The surface of (a) gibbsite before calcination, (b) gibbsite calcined at 260ºC, (c) gibbsite calcined at 450ºC and (d) gibbsite calcined at 470ºC

It can be seen in Figure 2 and Figure 3 that no crack can be found on the surface of gibbsite crystallite before calcination. The cracks appear at 260ºC, when the major phase of the sample converts from gibbsite to boehmite. Compared with gibbsite calcined at 260ºC, no obvious widening of the cracks is observed in gibbsite calcined at 450ºC. However, when calcination temperature rises to 470ºC, when boenmite convert to alumina, the cracks become significantly wider.

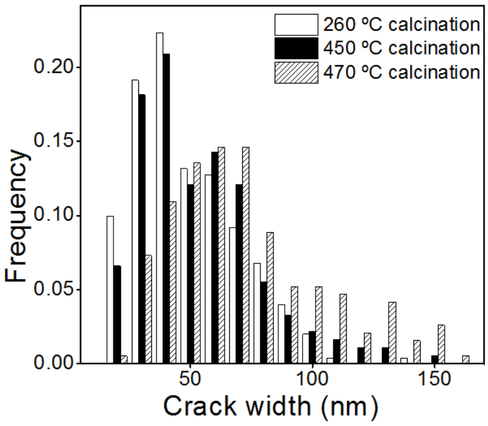

Figure 3. The width distribution of cracks on gibbsite calcined at different temperature

The linkage between calcination temperature, phase conversion and crack width change is summarised in Table 1.

Table 1. Summary of linkage between calcination temperature, phase conversion and crack width change

Calcination temperature change	**Room temperature to 260ºC**	**260ºC to 450ºC**	**450ºC to 470ºC**
Major phase conversion	Gibbsite to boehmite	Boehmite	Boehmite to alumina
Crack width change	Cracks appear	No significant change	Cracks widen

It can be seen that cracks appear on gibbsite crystallite surface at 260ºC, when the major phase converts from gibbsite to boehmite. With calcination temperature rises from 260ºC to 450ºC, the major phase remains to be boehmite and the width of crack does not change significantly, let alone the calcination temperature increases by 190ºC. However, with only another 20ºC increase, when calcination temperature reaches 470ºC and the major phaser converts from boehmite to alumina, a significant widening of crack can be observed. These results indicate that the generation and widening of crack is a step-wise process corresponding to the phase conversion. Therefore, it fortifies the idea that breakage of gibbsite crystallite during calcination is induced by the shrinkage of crystallite caused by the phase conversion happening in calcination.

To propose the mechanism of gibbsite crystallite breakage in calcination, we observed the internal structure of uncalcined gibbsite and gibbsite crystallite calcined at 260ºC, when the cracks first appear on the surface.

The picture of internal morphology of gibbsite and SGA calcined at 260ºC taken by FIB-SEM is presented in Figure 4.

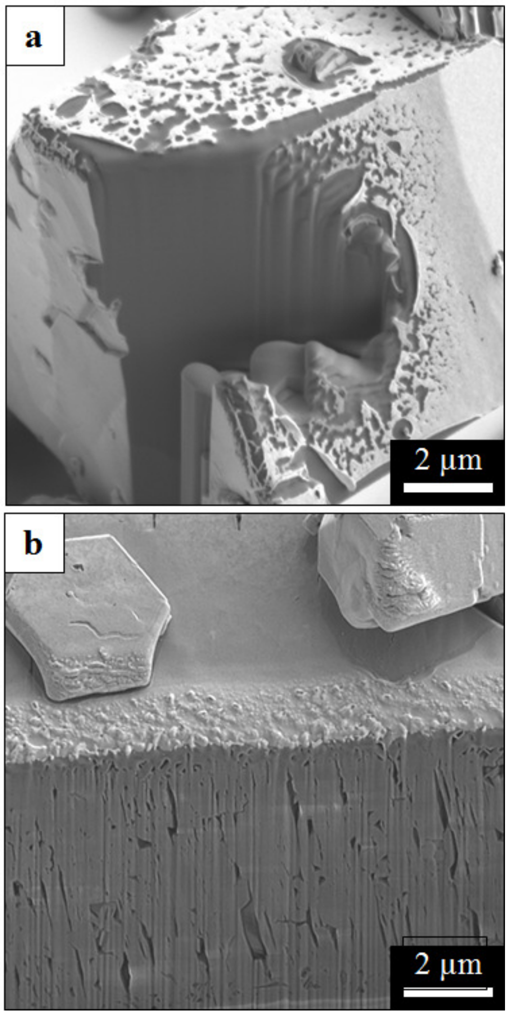

Figure 4. The FIB-SEM picture of internal morphology of (a) gibbsite without calcinetion and (b) gibbsite calcined at 260ºC

In Figure 4 (a), it is found that before calcination, the internal morphology of gibbsite is quite smooth and uniform. No crack or breakage is found in the bulk of the gibbsite crystallite. After calcination, in Figure 4 (b), cracks and pores appears in the bulk of the crystallite. Some strip-like cracks are found as well as some dot-like pores. The cracks are major strip-like and most of them are parallel with each other, and perpendicular to the c-axis of the crystallite. Meanwhile, the surface of the gibbsite crystallite remains relatively smooth. This indicates it is possible that cracks are firstly initiated in the bulk of gibbsite crystallite before calcination then some of them grow onto the surface.

To further prove that crystallites are generated in the bulk, we restricted the 3D tomography of gibbsite crystallite calcined, and presented in Figure 5.

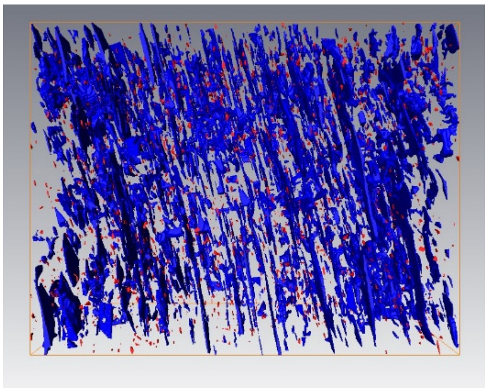

Figure 5. The typical 3D restructured distribution of internal cracks (blue) and crack seeds (red) in the crystallite of mosaic SGA calcined at 260ºC. The box size is 9.76 µm × 7.56 µm × 6.15 µm

In the 3D model of cracks and pores presented in Figure 5, the box size is 9.76 µm × 7.56 µm × 6.15 µm and he cracks are labelled blue and the pores red. The majority of cracks are found to be strip-like and parallel to each other which corresponds to the findings in Figure 4. The pores are found to distribute in different depth in the crystallite.

Most of cracks generated during calcination are found to be hidden beneath the surface in the bulk while the crystallite surface remains relatively smooth. This further illustrates that the cracks tends to generate firstly inside the bulk of crystallite and some of them can grow through the surface and become open cracks while most of these cracks remain inside the bulk.

To explain the reason why cracks are first generated inside the crystallite, we observed the cross-sectional morphology of calcined gibbsite, presented in Figure 6.

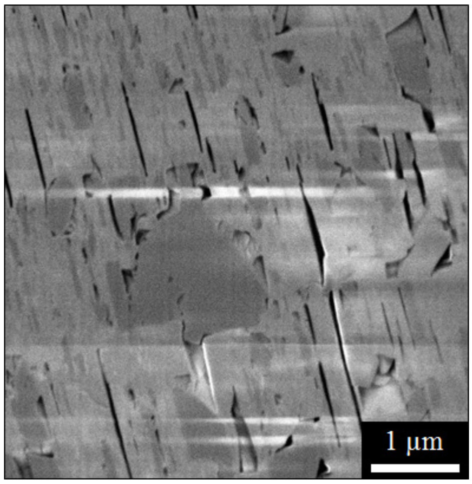

Figure 6. The back scattering SEM image of the cross-sectional morphology of gibbsite crystallite calcined at 260ºC

Due to the poor heat conductivity of gibbsite, the internal part of gibbsite crystallite remains partially calcined. The uncalcined part are shown as darker part in the back scattering SEM image. The interface can be a part accumulating the stress generated due to the shrinkage of the c-axis of gibbsite, therefore some cracks are found on the edge of the uncalcined part. These pores can further be a point accumulating the stress provided by further shrinkage of crystallite. With further calcination, the further generated stress can accumulate near these pores, leading to further breakage and generating cracks inside the bulk.

The mechanism of crack generation are given in Figure 7.

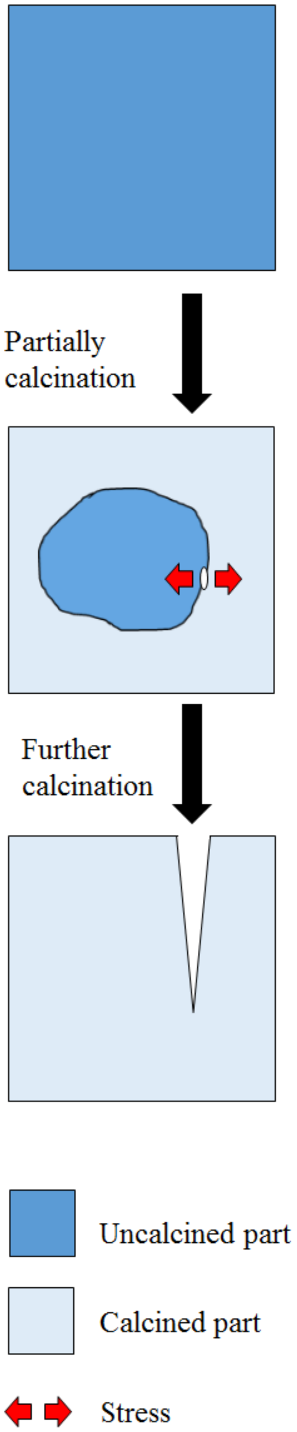

Figure 7. The mechanism of crack generation and growth

4. CONCLUSION

The generation and growth of cracks are found to be induced by phase conversion during calcination. Cracks tend to first generate inside the bulk as small pores on the interface between calcined part and uncalcined part inside the crystallite, then further grow to large crack. Understanding the process and mechanism of crack generation and growth can help to reduce the breakage in gibbsite calcination and reduce the content of ultra-fine particles.

5. ACKNOWLEDGEMENT

The author acknowledge the financial support from the Australian Research Council and South 32 Worsley Alumina Pty Ltd. The author also acknowledge the Centre of Microscopy and Microanalysis in The University of Queensland for the technological support. The Author offer special appreciation to Dr. Graeme Auchterlonie for support in TEM and Dr. Hui Diao for support in FIB.

6. REFERENCE

1. Linus Perander et.al. The nature and impacts of fines in smelter-grade alumina. *Jom* **2010,** *61* (11), 33-39.

2. Hasini Wijayaratne et.al. Relationships Between Smelter Grade Alumina Characteristics and Strength Determined by Nanoindentation and Ultrasound-Mediated Particle Breakage. *Metallurgical and Materials Transactions A* **2017,** *48* (6), 3046-3059.

3. Susanne Wind et. al. Development of particle breakdown and alumina strength during calcination. In *Light Metals 2010*, Johnson, J. A., Ed. 2010.

4. Martin Morgeneyer et.al. Experimental study of the aerosolization of fine alumina particles from bulk by a vortex shaker. *Powder Technology* **2013,** *246*, 583-589.

5. Eric AJM Boom. *Hydrate Toughness Development and Application: Breakage Index*; BHP Billiton Worsley Alumina Pty Ltd: 2014.

6. Linus Perander et.al. *Impact of calciner technologies on smelter grade alumina microstructure and properties*, The 8th International Alumina Quality Workshop, Darwin, Northern Territory, Australia, 2008.

7. J.V. Sang. Factors Affecting the Attrition Strength of Alumina Products. In *Light metals 1987*, Zabreznik, R. D., Ed. 1987.

8. Viktor Zsolt Baranyai et.al. Influence of The Short Time Grinding On the Thermal Decomposition Processes of Gibbsite Produced by The Bayer Process.

Materials Science and Engineering **2013,** *38/1* (15–27).

9. M. H. Stacey. Kinetics of Decomposition of Gibbsite and Boehmite and the Characterization of the Porous Products. *Langmuir* **1987,** *3* (5), 681-686.

10. L.Wang et.al. Shock-induced deformation of nanocrystalline Al: Characterization with orientation mapping and selected area electron diffraction. *Journal of Applied Physics* **2015,** *117* (084034), 1-10.